ELECTROLYTIC SEPARATION FACTORS OF HYDROGEN ON NICKEL

A Theoretical Estimate Allowing for Effects of Substrate Metal Atoms and Adsorbed Hydrogen

By

Juro HORIUTI[*] and Klaus MÜLLER[**]

(Received June 10, 1968)

Abstract

Potential energy maps, the coordinates of the critical complex, force constants, vibrational frequencies, activation energies, and separation factors for catalytic hydrogen combination on nickel: $2\,NiH \rightarrow Ni_2 + H_2$, were theoretically worked out. The effects of the underlying lattice plane of the metal has been fully accounted for, within the premises of the method,

(i) by varying the energy of the Ni–Ni bond on the basis of new data for the Ni_2 molecule, according to whether the system, $2\,Ni + 2\,H$, involves the nearest (2.49 Å), second-nearest (3.52 Å), or third-nearest (4.31 Å) two Ni atoms: this has pronounced effects on most of the quantities calculated, however, deuterium separation factors remain in the limits of 5.3 and 7.0;

(ii) by including the repulsion exerted on the two H atoms of the system $(2\,Ni + 2\,H)$ by up to third-nearest neighbouring Ni atoms in and below the metal surface plane for the (100), (110), and (111) lattice planes, for all configurations: this is the practical situation at zero coverage of the electrode with H atoms, $\theta_H = 0$;

(iii) by including the repulsion exerted on the two H atoms of the system $(2\,Ni + 2\,H)$ by hydrogen atoms adsorbed on the same surface Ni atoms as in (ii), for all configurations: this is the practical situation at unit coverage of the electrode with H atoms, $\theta_H = 1$.

The effects of repulsive interactions and the choice of crystal planes vary with the catalytic site considered. For the 2.49 Å site, surrounding metal atoms hardly affect the values of the activation energy and the electrolytic separation factors; surrounding hydrogen atoms lower the activation energy from 6 to 3 kcal/mole, but their effect on the separation factors is also slight; the deuterium separation factor remains approximately five. The crystal plane makes little difference in the effects.

For the 3.52 Å site, the effects due to repulsions depend more markedly on the crystal plane involved; activation energies are raised, and separation factors somewhat reduced, as compared to the situation of an isolated system, $2\,Ni + 2\,H$. Activation energies are relatively

 *) The Research Institute for Catalysis, Hokkaido University, Sapporo, Japan
 **) The Research Institute for Catalysis, Hokkaido University, Sapporo, Japan; present address: American Cyanamid Co., Stamford, Conn. 06904, U. S. A.

Juro HORIUTI and Klaus MÜLLER

high.

For the 4.31 Å site, the effects are drastic; the values for the energy of activation are prohibitively high.

Within the limits that are given by usual experimental error, calculated separation factors remain at values satisfactory for mechanistic diagnosis.

Introduction

In previous work[1-4], ROSEN and IKEHARA's calculations[5] were used to estimate the bond energy of the Ni_2 molecule. Now spectroscopic data have become available[6] from which the constants of the MORSE equation for Ni_2
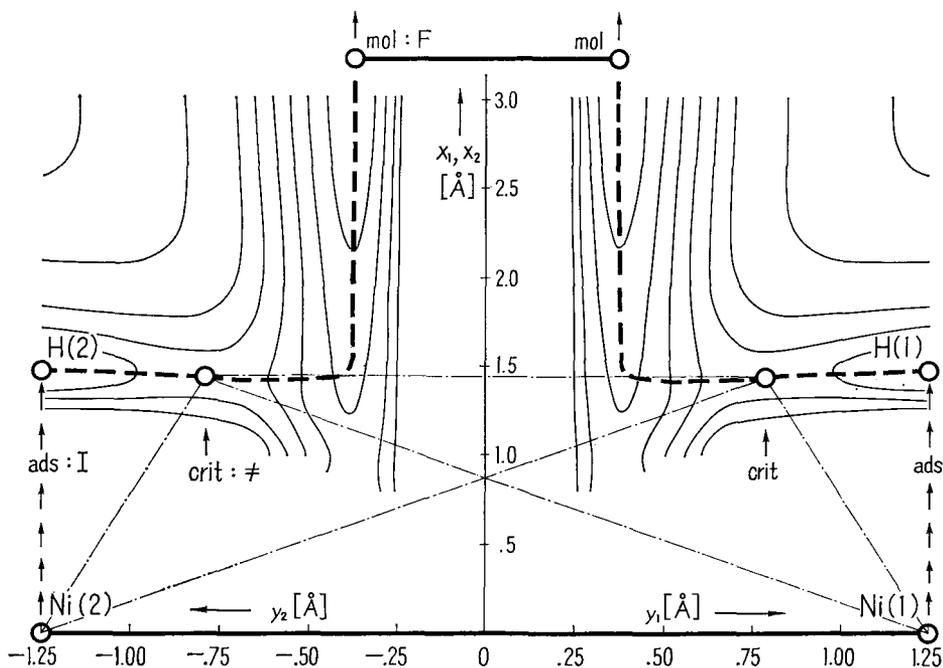

Figure 1. The system considered

Ni (1) and Ni (2) are two nickel atoms (here, for example, of site *I*), H (1) and H (2) are two hydrogen atoms adsorbed on them. Bold broken lines show schematically (without attention to its detailed course) the reaction path of catalytic combination of the two H atoms. This takes place in the plane $z = 0$ (the z-coordinate is normal to the plane of the paper), which leads from the initial state (I, the *adsorbed* hydrogen atoms) over the *critical* state ($\neq$) to the final state (F, *molecular* hydrogen). With solid lines, a typical potential energy map is indicated (see also figure 5; the potential energy coordinate is also normal to the plane of the paper). The configuration of I is indicated by vertical lines formed by arrows. The configuration of $\neq$ is indicated by dash-dotted lines. The configuration of F is indicated by bold solid lines; strictly, the molecular hydrogen should be at $x = \infty$.

can be found. It is possible, therefore, to assign Ni–Ni bond energies that depend on the Ni–Ni distance of the reaction site. Moreover, use of digital computers facilitates the numerical calculations involved, especially in the case where the effect of interactions between the two reacting H atoms and substrate metal atoms other than those of the reaction site, or between the reacting atoms and H atoms adsorbed on neighbouring sites, is to be determined for all configurations. Such calculations have been carried out in the present work.

System and data

The calculations refer to hydrogen atoms combining to molecules on a nickel substrate. The initial state is that of hydrogen atoms adsorbed on two adjacent surface Ni atoms. The reaction path is in a plane[7] normal to
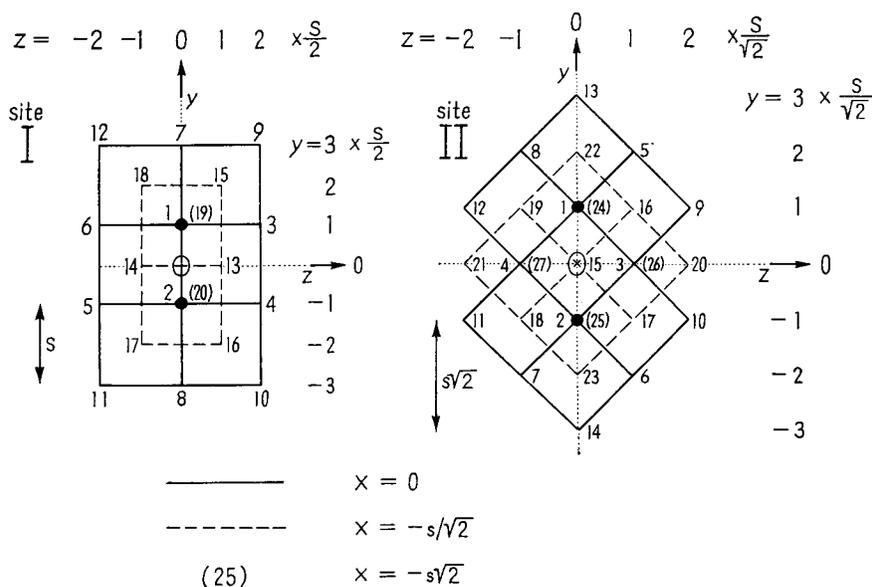
Figure 2. Sites on the (100) lattice plane

The nickel atoms taken into account in the calculations, and consecutively numbered, are in three planes parallel to the plane of the paper, at the intersections of the corresponding three grids of solid or broken lines, and have the coordinates x (normal to the plane of the paper, common for each plane, and explained at the bottom of the figure; $x=0$ is the surface plane of the metal), y (the ordinate, with divisions as shown from top to bottom to the right of each part of the figure), and z (the abscissa, with divisions as shown from left to right on top of each part of the figure). The two nickel atoms forming the catalytic site (Ni (1) and Ni (2)) are indicated by full circles; their distance apart $(y_1 - y_2)$ is shown as a double-headed arrow. $s = 2.492$ Å.

Juro HORIUTI and Klaus MÜLLER

the metal surface[1]. The final state is the free hydrogen molecule. The nickel surface is, or is not, covered with H atoms in the r-state[8]. Nearest, second-nearest, and third-nearest neighbours are selected, and coordinates assigned, as shown in figures 1–4. The origin of the coordinate system is at the
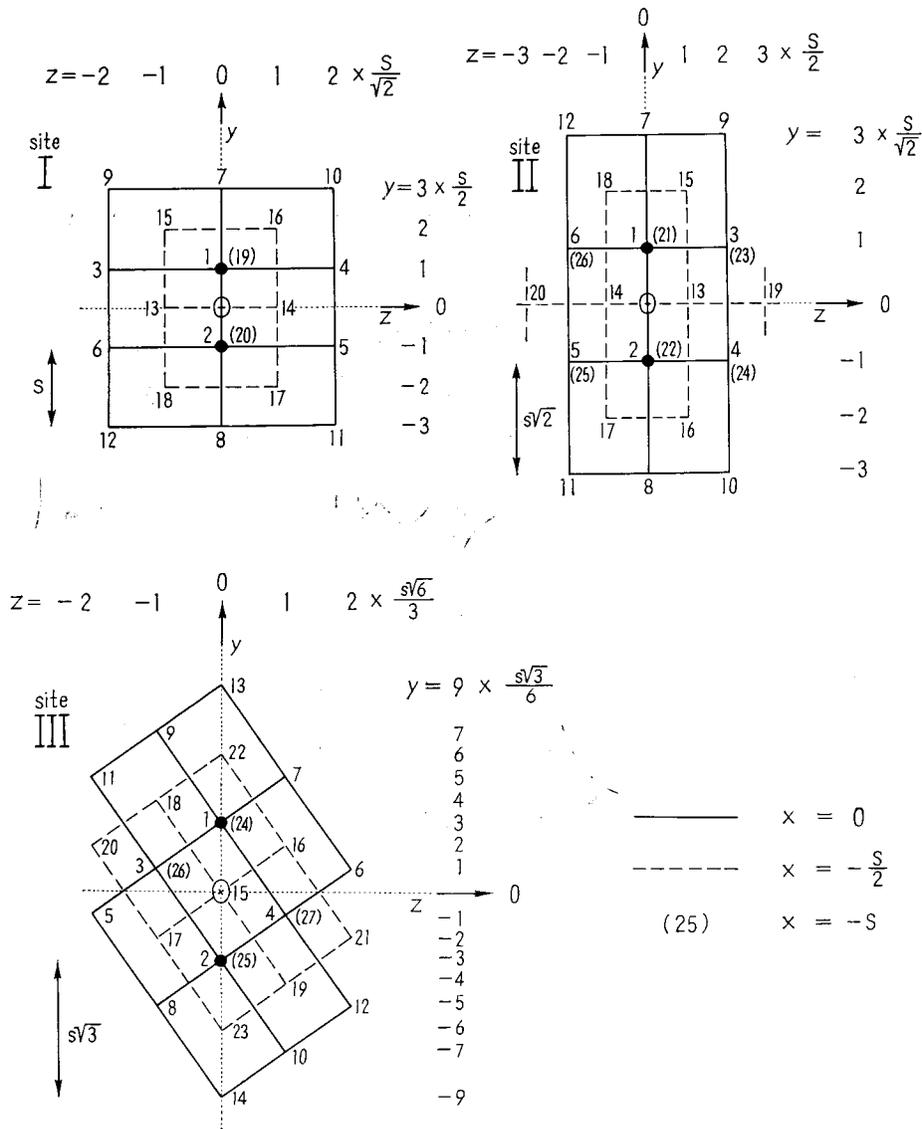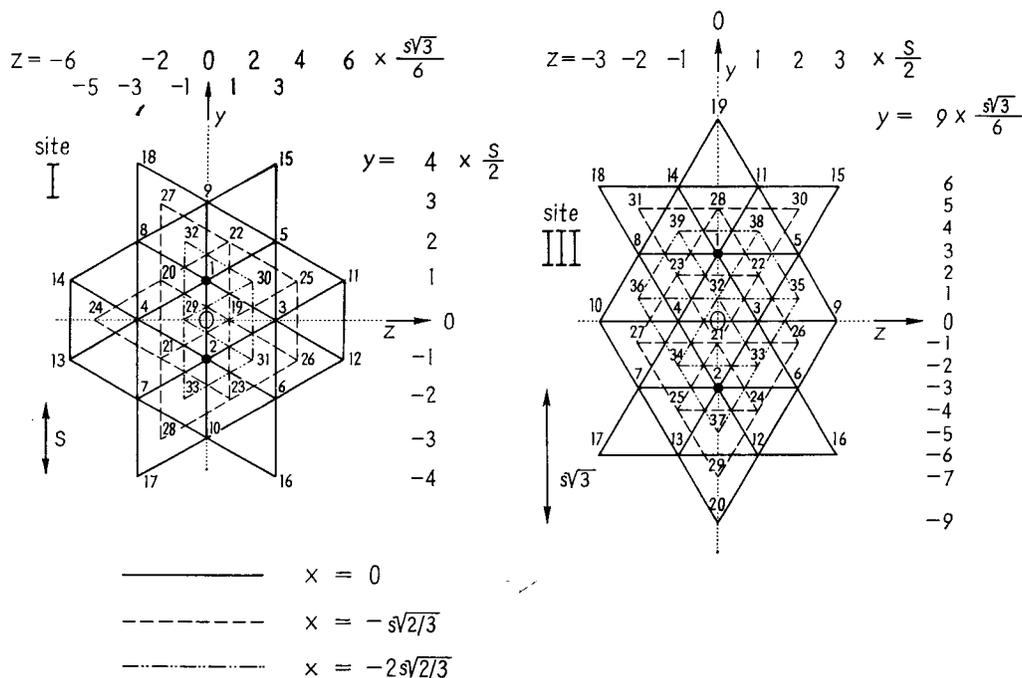

Figure 3. Sites on the (110) lattice plane
Details as in figure 2.

midpoint of the line connecting the two Ni atoms forming the catalytic reaction site. These Ni atoms are 2.492, 2.492 $\sqrt{2}$, and 2.492 $\sqrt{3}$ Å apart[9]. Such sites, referred to in the following as *I*, *II*, and *III*, respectively, are on the (100), (110), and (111) planes as substrate surfaces, see figures 2 to 4 and table 1. The MORSE function for all bonds involved is

$$K + J = D \left(\exp\left(-2a(r - r_0) \right) - 2 \exp\left(-a(r - r_0) \right) \right) \qquad (1)$$

Figure 4. Sites on the {111} lattice plane
Details as in figure 2.

TABLE 1. The 17 cases considered

Site	Ni–Ni distance	Number of interacting atoms adjacent to the system, $2\,\mathrm{Ni} + 2\,\mathrm{H}$, taken into account						
		NET	MAE			HAE		
			(100)	(110)	(111)	(100)	(110)	(111)
I	2.492 Å	0	18 Ni	18 Ni	31 Ni	18 Ni 10 H	18 Ni 10 H	31 Ni 16 H
II	2.492 $\sqrt{2}$ Å	0	25 Ni	24 Ni	—	25 Ni 12 H	24 Ni 10 H	— —
III	2.492 $\sqrt{3}$ Å	0	—	25 Ni	37 Ni	— —	25 Ni 12 H	37 Ni 18 H

where K and J are the COULOMB and exchange integrals, respectively, D is the dissociation energy, a is the MORSE constant, r_0 the equilibrium distance, and r the distance. The values used for D, a, and r_0, and the percentages assigned to K and J are shown in table 2.

TABLE 2. Data

Molecule	Internucl. dist. (Å)	r_0, equil. dist. (Å)	D, dissoc. energy (kcal/mole)	K, Coul. energy (% of D)	J, exch. energy (% of D)	a, Morse const. (Å^{-1})
Ni-Ni	2.49	—	51.41	37	63	—
	3.52	—	15.53	37	63	—
	4.31	—	4.87	37	63	—
	r_0	2.30	55.0	—	—	1.535
Ni-H	r_0	1.48	60.0	24	76	1.600
H-H	r_0	.742	109.52	11	89	1.943

The calculations have been done in three stages: NET (the system, $2\,\text{Ni} + 2\text{H}$, alone, the only substrate effect being the invariance of the coordinates of the two Ni atoms involved), MAE (the same as NET, but including the repulsion exerted on the system by the underlying metal atoms, for brevity referred to as "Metal Atom Effect"), and HAE (the same as MAE, but also including the repulsion exerted on the system by the surrounding adsorbed hydrogen atoms, for brevity referred to as "Hydrogen Atom Effect"). MAE corresponds to zero coverage of the electrode with hydrogen, HAE to unit coverage. Table 1 details the 17 cases that result, according to the availability of sites I, II, and III on the three lattice planes considered, in terms of the numbers of interacting atoms in each stage.

Potential energy maps

Under the assumption that only the two H atoms of the system, $2\,\text{Ni} + 2\text{H}$, move during the reaction, whose coordinates are (x_1, y_1) and (x_2, y_2), and further, that their motion along the reaction path is always such that

$$x_1 = x_2, \quad y_1 = -y_2, \quad z_1 = z_2 = 0,$$

one can choose the coordinates

$$x = \frac{x_1 + x_2}{2} \quad \text{and} \quad y = \frac{y_1 - y_2}{2}$$

as independent variables in calculating the potential energy of the system,

$E = E(x, y)$; see figure 1. This is given by (*cf.* the equations III. 2 and III. 3 of HORIUTI and KITA[4])

$$E = FK + FJ, \qquad \text{(cases NET)}$$
$$E = FK + FJ + RM, \qquad \text{(cases MAE)} \qquad (2)$$
$$E = FK + FJ + RM + RH, \qquad \text{(cases HAE)}$$

where FK represents COULOMB integrals, and FJ exchange integrals, for the four atoms of the system, RM the terms expressing the metal atom effect, and RH the terms expressing the hydrogen atom effect, thus:

$$FK = K_{M1M2} + K_{H1H2} + K_{M1H1} + K_{M2H2} + K_{M1H2} + K_{M2H1},$$
$$K_{M1H1} = K_{M2H2},$$
$$K_{M1H2} = K_{M2H1},$$
$$FJ = -0.7071 \left((\alpha - \beta)^2 + (\beta - \gamma)^2 + (\gamma - \alpha)^2\right)^{1/2},$$
$$\alpha = J_{M1M2} + J_{H1H2},$$
$$\beta = J_{M1H1} + J_{M2H2},$$
$$\gamma = J_{M1H2} + J_{M2H1},$$
$$J_{M1H1} = J_{M2H2},$$
$$J_{M1H2} = J_{M2H1},$$
$$RM = \sum_i (K_i - (1/2)J_i),$$
$$K_i = K_{MiH1} + K_{MiH2},$$
$$J_i = J_{MiH1} + J_{MiH2},$$
$$RH = \sum_j (K_j - (1/2)J_j),$$
$$K_j = K_{HjH1} + K_{HjH2},$$
$$J_j = J_{HjH1} + J_{HjH2},$$

where M1, M2, and Mi are to represent Ni(1), Ni(2) (see figure 1), and Ni(i) (see figures 2 to 4), H1, H2, and Hj are H(1), H(2) (see figure 1), and hydrogen atoms adsorbed on Ni(i) located in the surface plane; $\sum_i$ takes the sum[*] over all underlying Ni atoms shown, except Ni(1) and Ni(2), $\sum_j$ takes the sum[*] over all adsorbed hydrogen atoms except H(1) and H(2); and the K and J with designations for two atoms in the suffix are defined by equation (1) and table 2, with the distances $(r - r_0)$ expressed through the coordinates of any two interacting atoms as functions of x and y. FORTRAN programmes were written for use by the computers NEAC-2203 G (Nippon Electric) of Hokkaido University and HITAC-5020 (Hitachi) of Tokyo University. Input data were those of table 2, further the coordinates of the metal atoms shown in figures 1 to 4, and the coordinates of the hydrogen atoms adsorbed on surface Ni atoms for which $x_{Hj} = r_0$ (Ni-H), while y_{Hj} and z_{Hj} are numerically equal to y_{Mi} and z_{Mi} for $j = i$.

---

[*] The number of terms in each case can be seen from table 1.

Juro HORIUTI and Klaus MÜLLER

NET I

NET I

Fig. 5a 5b

MAE I (100)

MAE I (100)

Fig. 6a 6b

HAE I (100)

HAE I (100)
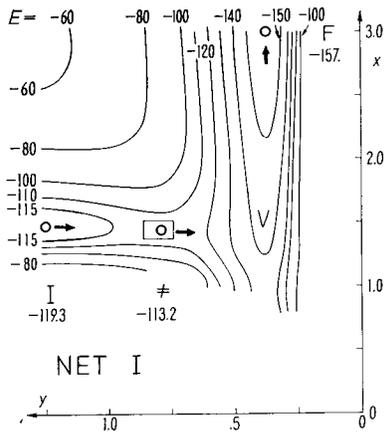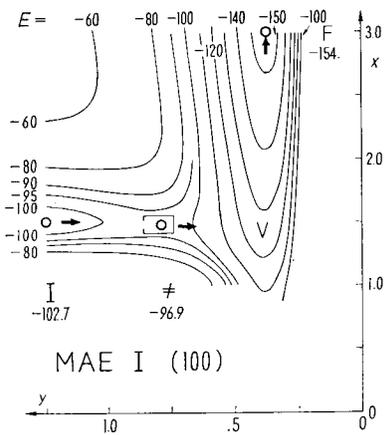
Fig. 7a 7b

Electrolytic Separation Factors of Hydrogen on Nickel

Fig. 8a 8b

Fig. 9a 9b
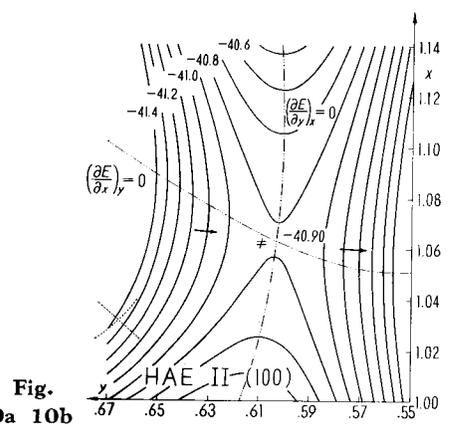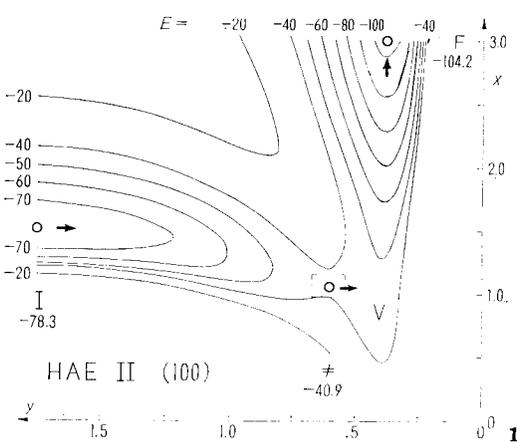
Fig. 10a 10b

Fig. 11a

Fig. 12a

Fig. 13a

Electrolytic Separation Factors of Hydrogen on Nickel

Fig. 11b

Fig. 12b

Fig. 13b

Juro HORIUTI and Klaus MÜLLER
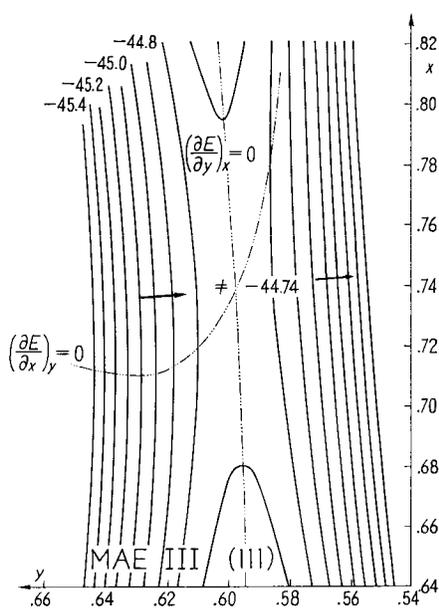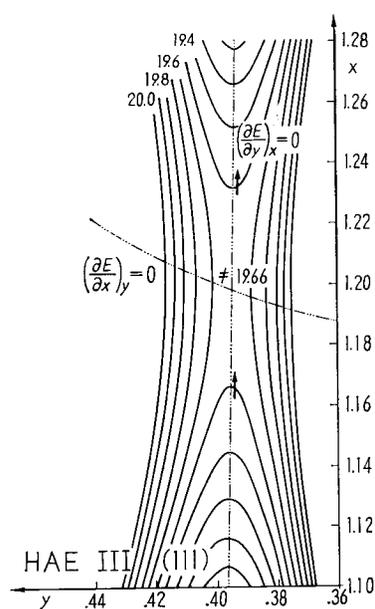
Table 3 gives some numerical examples for the terms entering RM and RH. Their rapid decrease as a function of distance is a justification f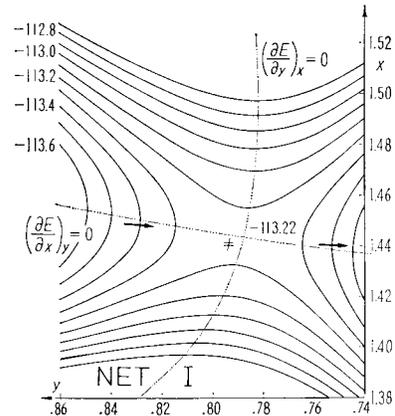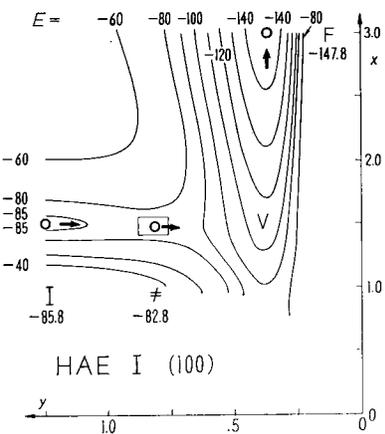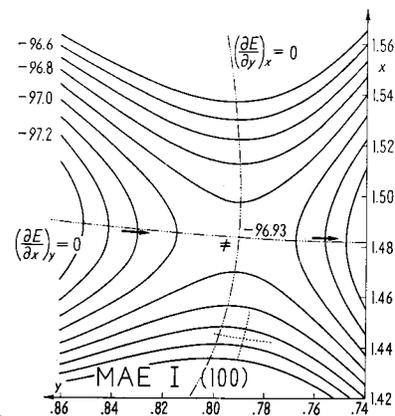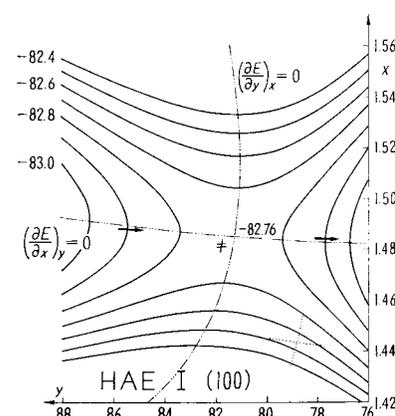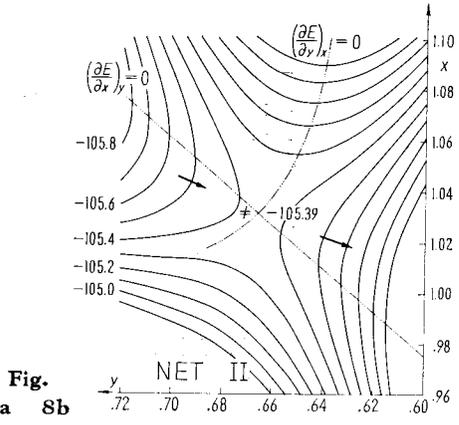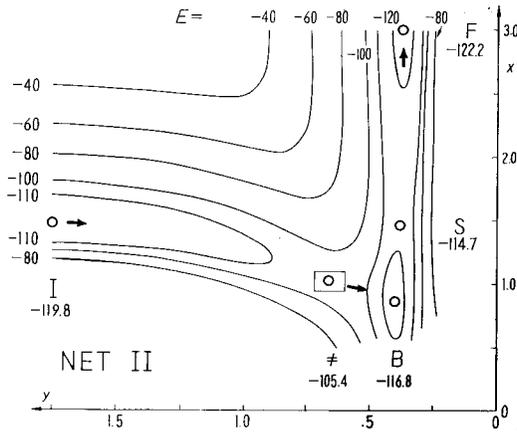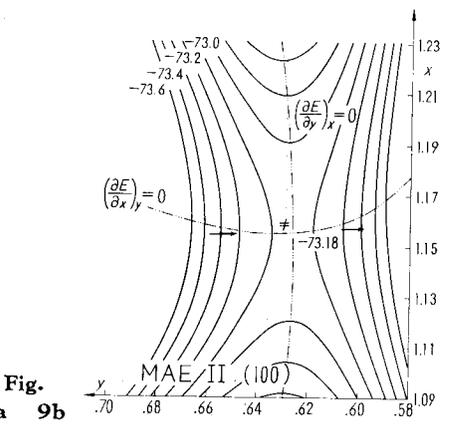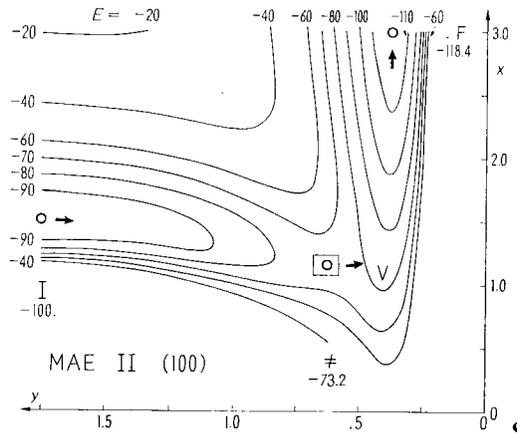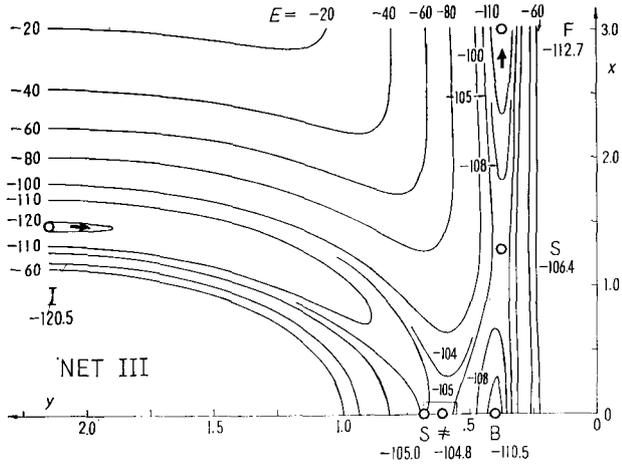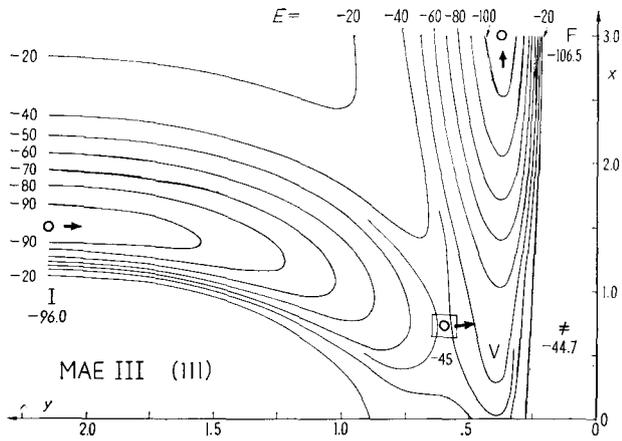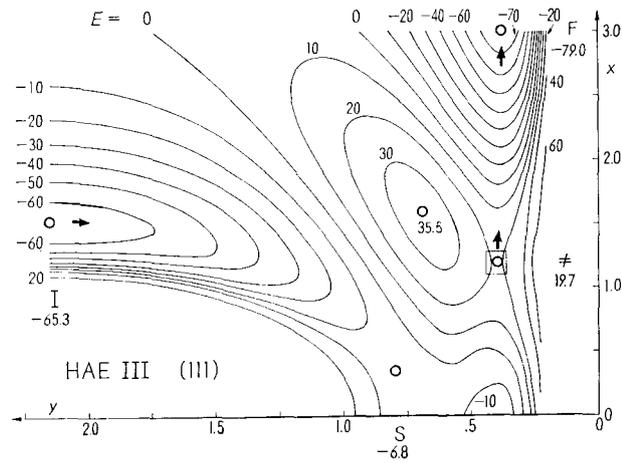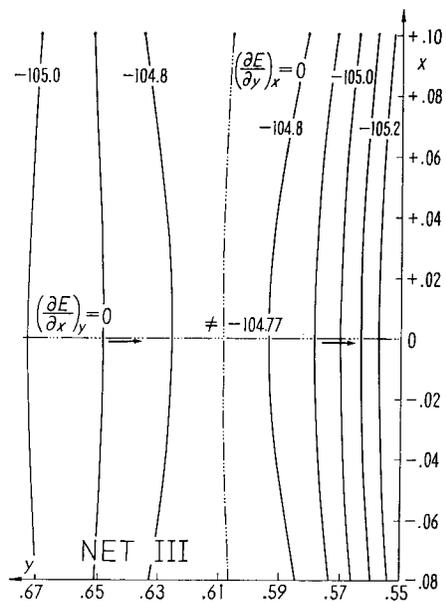or not extending the summation over a greater number of surrounding atoms. They also confirm TAFEL's early observation (Ref. 10, in a footnote !) that a monolayer or so of a material suffices to show the essential catalytic effects of that material.

TABLE 3. Examples for the terms $(K_i - (1/2) J_i)$

Atom pair (1–2)	$y_1 - y_2$ (Å)	$x_1 - x_2$ (Å)	distance (Å)	$(K_i - (1/2) J_i)$ (kcal/mole)
H–Ni	2.49	1.48	2.89	1.67
	3.52	1.48	3.82	.39
	4.31	1.48	4.56	.12
H–H	2.49	0	2.49	2.4
	3.52	0	3.52	.32
	4.31	0	4.31	.07

The data output $E = E(x, y)$ was plotted as $E = E(x)$ and $E = E(y)$, and for even values of E, sufficient coordinates were read to plot the potential energy maps which are shown in figures 5 a to 13 a. The computer cal-

Figures 5 a to 13 a. Potential eneryg surfaces
The potential energy surfaces for the cases indicated in each figure are plotted on identical scales. I is the initial state, at $y = y_{Ni(1)} = - y_{Ni(2)}$; ≠ is the critical state; F is the system approaching a final state (arbitrarily shown at $x = 3$ Å). The designated areas around the saddle point are shown on an expanded scale in figures 5 b to 13 b. B designates a basin in the potential energy surface. S are those saddle points that are not the highest points in a given reaction path, and which have been disregarded (in the case of figure 13 a, this is perhaps not in principle a valid procedure; however, S (−6.8) is not a well-defined saddle point, its surroundings being a rather flat surface).
Several cases are not shown among the diagrammes, because they are similar to others that are shown. Thus, MAE and HAE I (100) (figures 6 and 7) do not differ much from MAE and HAE I (110) and (111), respectively; MAE and HAE II (100) (figures 9 and 10) are similar to MAE and HAE II (110); and MAE III (111) (figure 12) is similar to both MAE and HAE III (110).

Figures 5 b to 13 b. Potential energy surfaces near ≠
Potential energy surfaces in the vicinity of the saddle points are given for the same cases as shown in figures 5 a to 13 a. The dash-dotted lines $(\partial E/\partial y)_x = 0$ and $(\partial E/\partial x)_y = 0$ intersect at the saddle point ≠ but *do not elsewhere coincide with the reaction path*; the approximate path of the system is indicated by arrows. The small portions of broken lines in figures 6 b, 7 b and 10 b indicate, for comparison, the location of the saddle point in the corresponding NET cases. (In other cases, this is outside the area shown.)

culations were then repeated for the regions around the saddle point as seen from the first set of maps, with more closely spaced values of x and y, to obtain the detailed maps as shown in figures 5 b to 13 b. The maxima and minima, respectively, of the detailed plots of $E(x)$ and $E(y)$ were determined graphically, plotted, and used to find accurately the coordinates of the saddle point, which is their point of intersection, as shown in the figures; analogous plots were also used to find accurately the energy of the critical complex. Table 4 gives saddle point coordinates and energies.

TABLE 4. Saddle point data[*]

Site	Data	NET	MAE			HAE		
			(100)	(110)	(111)	(100)	(110)	(111)
I (2.49 Å)	$x^{\neq}$ (Å)	1.444	1.484	1.475	1.494	1.485	1.476	1.495
	$y^{\neq}$ (Å)	.788	.790	.790	.788	.813	.807	.791
	$-E^{\neq}$ (kcal/	113.22	96.93	101.80	92.37	82.76	97.79	69.43
	E_A mole)	6.1	5.8	6.3	6.4	3.0	3.0	4.7
II (3.52 Å)	$x^{\neq}$ (Å)	1.031	1.155	1.120	—	1.064	1.111	—
	$y^{\neq}$ (Å)	.666	.626	.636	—	.603	.643	—
	$-E^{\neq}$ (kcal/	105.39	73.18	83.59	—	40.90	76.23	—
	E_A mole)	14.4	26.8	21.7	—	37.4	18.6	—
III (4.31 Å)	$x^{\neq}$ (Å)	.000	—	.873	.738	—	.707	1.198
	$y^{\neq}$ (Å)	.609	—	.607	.598	—	.587	.395
	$-E^{\neq}$ (kcal/	104.77	—	61.47	44.74	—	46.70	−19.66
	E_A mole)	15.7	—	42.0	51.3	—	46.1	85.0

[*] E_A is the difference between the energies of the system at $\neq$ $(E^{\neq})$ and I (the initial state in each case—not to be confused with site *I*), disregarding any zero point vibrational energies.

Force constants and vibrational frequencies of the critical complex

The force constants, a_{qq}, of the critical complex were found as second derivatives of E with respect to the new coordinates (x and y were defined above):

$$x = \frac{x_1 + x_2}{2} \qquad \xi = \frac{x_1 - x_2}{2}$$

$$y = \frac{y_1 - y_2}{2} \qquad \eta = \frac{y_1 + y_2}{2}$$

Juro HORIUTI and Klaus MÜLLER

$$z = \frac{z_1 - z_2}{2} \qquad \zeta = \frac{z_1 + z_2}{2},$$

where again suffixes 1 and 2 refer to H(1) and H(2), respectively, see figure 1. The saddle point is, in these coordinates, at $(x^{\neq}; y^{\neq};$ and $z^{\neq} = \xi^{\neq} = \eta^{\neq} = \zeta^{\neq} = 0)$. The energy of the system near the saddle point is expressed as

$$E = E^{\neq} + \frac{1}{2} \sum_q a_{qq}(q - q^{\neq})^2 + a_{xy}(x - x^{\neq})(y - y^{\neq}) + a_{\xi\eta}\xi\eta, \qquad (3)$$

TABLE 5. Force constants of the critical complexes

Site	Force constant (kcal/ mole·Å)	NET	MAE			HAE		
			(100)	(110)	(111)	(100)	(110)	(111)
I (2.49 Å)	a_{xx}	339.32	332.25	349.75	312.05	344.30	363.78	295.85
	$a_{\xi\xi}$	441.78	383.09	398.30	366.67	384.04	404.14	349.06
	a_{yy}	−236.66	−248.37	−243.48	−258.57	−184.68	−193.23	−240 01
	$a_{\eta\eta}$	69.00	70.92	71.32	71.43	75.20	77.38	82.14
	a_{zz}	35.20	57.12	48.87	63.73	82.42	46.17	116.28
	$a_{\zeta\zeta}$	.02	20.16	12.59	24.99	55.19	17.20	78.91
	a_{xy}	−62.83	−19.88	−29.15	−7.62	−30.31	−36.42	−8.25
	$a_{\xi\eta}$	−103.23	−76.83	−82.36	−69.44	−79.41	−84.19	−69.28
II (3.52 Å)	a_{xx}	223.53	128.30	160.75	—	122.53	168.16	—
	$a_{\xi\xi}$	270.08	239.22	251.31	—	245.61	248.71	—
	a_{yy}	−194.64	−568.00	−473.67	—	−525.27	−427.14	—
	$a_{\eta\eta}$	280.26	150.82	183.18	—	182.87	196.74	—
	a_{zz}	44.33	131.15	109.32	—	218.28	118.30	—
	$a_{\zeta\zeta}$	−.12	34.08	28.50	—	103.24	46.14	—
	a_{xy}	−190.90	10.20	−40.63	—	−53.99	−59.50	—
	$a_{\xi\eta}$	−220.43	−82.60	−114.98	—	−124.74	−126.77	—
III (4.31 Å)	a_{xx}	12.10	—	40.02	19.08	—	37.79	−108.72
	$a_{\xi\xi}$	93.88	—	185.70	156.16	—	187.20	65.14
	a_{yy}	−244.18	—	−846.76	−777.60	—	−772.52	2083.34
	$a_{\eta\eta}$	389.91	—	77.33	103.58	—	111.92	−66.03
	a_{zz}	93.88	—	177.04	97.12	—	219.53	262.09
	$a_{\zeta\zeta}$	12.10	—	44.57	−31.61	—	77.97	100.99
	a_{xy}	.00	—	104.46	41.52	—	61.31	42.77
	$a_{\xi\eta}$	.00	—	.43	−39.88	—	−18.28	1.56

where q stands for any of the six new coordinates. Analytical expressions were derived from equation (2) for the eight force constants, by double differentiation with respect to the coordinates or combinations of coordinates required. A FORTRAN programme was written for use by the computer NEAC–2203 G of Hokkaido University. With the same data input as above (calculation of the potential energy maps), and in addition with the coordinates of the critical complex, force constants for the 17 cases of table 1 were calculated; they are given in table 5.

Lastly, a Library Programme (M4401) was used in writing a third FORTRAN programme to produce from an input of force constants a symmetric matrix, and then solve the symmetrical secular equations

TABLE 6. Vibrational frequencies and partition
functions of $(H-H)$

Site	$\nu_i{}^{\rm ll}$ (cm^{-1}) and $f_{\rm H}^{\neq}$	NET	MAE			HAE		
			(100)	(110)	(111)	(100)	(110)	(111)
I (2.49 Å)	ν_1	1655.3	1531.4	1563.4	1495.1	1535.8	1575.8	1463.1
	ν_2	1540.0	1395.5	1433.2	1351.2	1422.6	1463.4	1315.7
	ν_3	497.5	557.0	550.1	571.9	572.2	577.2	617.7
	ν_4	453.7	578.0	534.6	610.5	694.3	519.7	824.7
	ν_5	10.8	343.4	271.4	382.3	568.2	317.2	679.4
	ν_6 (i)	1191.7	1206.9	1196.9	1230.0	1044.2	1069.6	1185.1
	$f_{\rm H}^{\neq} \cdot 10^5$	107.	3.42	4.39	3.20	1.12	3.19	.82
II (3.52 Å)	ν_1	1702.7	1299.5	1404.3	—	1416.1	1435.1	—
	ν_2	1319.3	866.8	977.4	—	861.9	1009.0	—
	ν_3	565.5	769.9	754.5	—	707.6	738.8	—
	ν_4	509.2	875.8	799.6	—	1129.9	831.8	—
	ν_5	7.7	446.5	408.3	—	777.1	519.5	—
	ν_6 (i)	26.5	1822.9	1669.0	—	1760.2	1591.5	—
	$f_{\rm H}^{\neq} \cdot 10^5$	162.	4.13	3.46	—	.81	2.04	—
III (4.31 Å)	ν_1	741.0	—	1042.2	1019.3	—	1058.1	617.3
	ν_2	266.0	—	552.3	352.4	—	498.0	3491.5
	ν_3	1510.2	—	672.5	693.0	—	793.7	1238.1
	ν_4	741.0	—	1017.6	753.7	—	1133.1	768.6
	ν_5	266.0	—	510.6	254.3	—	675.3	452.4
	ν_6 (i)	1195.1	—	2241.4	430.0	—	2132.0	621.5
	$f_{\rm H}^{\neq} \cdot 10^5$	41.	—	13.1	112.	—	5.19	.016

Juro HORIUTI and Klaus MÜLLER

$$\begin{vmatrix} b_1(a_{xx}+a_{\xi\xi})-\lambda & b_3(a_{xx}-a_{\xi\xi}) & b_1(a_{xy}+a_{\xi\eta}) & b_3(a_{xy}-a_{\xi\eta}) \\ & b_2(a_{xx}+a_{\xi\xi})-\lambda & b_3(a_{xy}-a_{\xi\eta}) & b_2(a_{xy}+a_{\xi\eta}) \\ & & b_1(a_{yy}+a_{\eta\eta})-\lambda & b_3(a_{yy}-a_{\eta\eta}) \\ & & & b_2(a_{yy}+a_{\eta\eta})-\lambda \end{vmatrix}=0$$

and

$$\begin{vmatrix} b_1(a_{zz}+a_{\zeta\zeta})-\lambda & b_3(a_{zz}-a_{\zeta\zeta}) \\ & b_2(a_{zz}+a_{\zeta\zeta})-\lambda \end{vmatrix}=0$$

where $\quad b_1 = 1/4\,m_1$,

$\qquad b_2 = 1/4\,m_2$,

$\qquad b_3 = 1/(m_1 m_2)^{1/2}$,

$\qquad \lambda = 4\pi^2(\nu^{\neq})^2$,

m_1 is the mass of H(1), m_2 is the mass of H(2), one of these hydrogen atoms being ^1H, the other ^1H, $^2H = D$, or $^3H = T$, and $\nu^{\neq}$ are the six vibrational frequencies (five real and one imaginary) of the critical complex in each case. These frequencies are listed in table 6. The vibrational partition functions at 298 °K were obtained in the same computer calculation, and used to find the separation factors.

Separation factors

These are given by[1], excluding the quantum correction,

$$S_D = \frac{f_H^{\neq}}{f_D^{\neq}} \frac{f_{HDO,g}}{f_{H_2O,g}} K_D \quad \text{and} \quad S_T = \frac{f_H^{\neq}}{f_T^{\neq}} \frac{f_{HTO,g}}{f_{H_2O,g}} K_T$$

where

$$K_D = \frac{a_{HDO,l} \cdot a_{H_2O,g}}{a_{H_2O,l} \cdot a_{HDO,g}} \quad \text{and} \quad K_T = \frac{a_{HTO,l} \cdot a_{H_2O,g}}{a_{H_2O,l} \cdot a_{HTO,g}}$$

are equilibrium constants for exchange between the liquid (l) and gas (g) phases (their numerical values are 1.07[11] and 1.093[12], respectively), a are activities, and f are partition functions whose ratios

$$f_{HDO,g}/f_{H_2O,g} = 59.16$$

and

$$f_{HTO,g}/f_{H_2O,g} = 289.54$$

were calculated by SRINIVASAN[13] from spectroscopic data[14,15]; further,

$$\frac{f_H^{\neq}}{f_D^{\neq}} = \frac{1}{2} \frac{\prod_i(\sinh(h\nu_i^D/2kT))}{\prod_i(\sinh(h\nu_i^H/2kT))}$$

and

$$\frac{f_H^{\neq}}{f_T^{\neq}} = \frac{1}{2} \frac{\prod_i(\sinh(h\nu_i^T/2kT))}{\prod_i(\sinh(h\nu_i^H/2kT))} \, ,$$

where the product is taken over the five real vibrational frequencies, ν_i, of the respective isotopes in the critical complexes concerned. The separation factors are given in table 7.

TABLE 7.   Separation factors (excl. tunnelling correction)

Site	Sep. factors	NET	MAE			HAE		
			(100)	(110)	(111)	(100)	(110)	(111)
I	S_D	5.29	5.42	5.41	5.47	4.98	5.30	4.90
(2.49 Å)	S_T	10.85	11.27	11.23	11.43	10.09	10.93	9.85
II	S_D	6.71	5.88	5.69	—	4.92	5.44	—
(3.52 Å)	S_T	16.16	12.54	12.02	—	9.84	11.31	—
III	S_D	6.98	—	6.78	9.66	—	6.08	3.66
(4.31 Å)	S_T	16.27	—	15.35	26.00	—	13.16	7.19

Discussion

Previous calculations*) have revealed a very strong effect of repulsive interactions between the critical complex and surrounding adatoms on the theoretical values of the rates (incl. the limiting rates) of the hydrogen electrode reaction[1,4,16,18-21], its TAFEL slope[1,4,19,21-23] **), activation energy[1,4,19,24,25] and pH dependence[23], as well as a strong effect of the same type of interactions between the adatoms themselves on the adsorption behaviour (shape of the isotherms[4,26-32], heats of adsorption[1,27,35-37] ***), entropy of adsorption[37], pseudo capacity[38,39], and the state of adsorption of the adsorbed hydrogen species[40] ****)

---

  *) For summaries, see references 16 and 17.

 **) In Ref. 22, such interactions may be taken as implicitly accounted for with the use
        of a corresponding empirical isotherm.

***) HABER and RUSS[33] have first pointed out that there may well be a requirement for
        additional work due to deviations from the ideal gas law when the adsorbed gas
        film, during H_2 evolution, must be replenished continuously.   TAFEL[34] referred to
        their work when he attributed anomalies in the TAFEL slope to concentrated
        solution type behaviour of the gas film, *i.e.*, implicitly, interactions.

****) Particularly in the case of platinum, much less in the case of nickel.

for hydrogen adsorbed on a metal. It remained to be shown if there is a strong effect of these same interactions on the expected values of separation factors. If so, the diagnostic value of separation factors[17,41-43] would decline considerably.

Table 4 shows an appreciable effect of the substrate on the coordinates of the critical system only where the Ni–Ni distance is varied, but not where the lattice plane is changed*), while the saddle point energy and the activation energy of the combination step (as given in the same table) are considerably affected in all cases by the interactions with surrounding atoms. Tables 5 and 6 (see particularly the values for the partition functions) likewise demonstrate the importance of interactions. However, table 7 indicates that there is a rather *moderate effect* in all but two**) of the seventeen cases investigated, where *separation factors* are concerned. The significance of any effects of interactions on separation factors is, moreover, further reduced when it is seen that, because of the relative values of the energies of activation, the combination reaction is sufficiently probable only on Ni atoms 2.49 Å apart (sites *I*), where the effects are smallest. All deuterium separation factors for the reaction on these sites are, for example, between 4.9 and 5.5, while the value for the system without interactions (NET) is 5.3 (all values without tunnelling correction). Such a variation is within usual experimental errors.

The effects are now discussed in more detail.

1. The coordinates of the saddle point

In table 8, the present results are compared with those of other recent authors[3,4], all obtained in absence of interactions. Considerable deviations are indicated for sites *I* and *III*. In previous work, D_{Ni-Ni} has been taken as 20 or 20.6 kcal/mole; this value is rather close to D_{Ni-Ni} for site *II* used in the present work (see table 2), and there is hence little change in the saddle point coordinates between previous calculations and the present ones for sites *II*. It cannot be concluded, however, as done previously[3], that a variation of the metal-metal distance does not strongly affect the results.

It may be mentioned in passing that even on the basis of ROSEN and IKEHARA's work, distance-variant bond energies might have been calculated, by making the appropriate readings from their plots at different values of their distance parameter ρ; the result of doing so is a decrease in the Ni–Ni bond energy from, *e. g.*, 21.9 kcal for site *I* to 8.4 kcal for site *II* and to 6 kcal for site *III*, approximately.

---

*) With the exception of one case, as discussed below.
**) The cases *III*, MAE and HAE, on the (111) plane; see below for details.

TABLE 8.   Comparison with previously published results

Site	Data	HORIUTI and KITA[4]	BOCKRIS and SRINIVASAN[3]	Present work (NET)	Present work (HAE (110))
I (2.49 Å)	$x^{\neq}$ (Å)	1.400	1.74	1.444	1.476
	$y^{\neq}$ (Å)	.635	.39	.788	.807
	S_D		5.9	5.29	5.30
II (3.52 Å)	$x^{\neq}$ (Å)	1.040	1.06	1.031	1.111
	$y^{\neq}$ (Å)	.676	6.9	.666	.643
	S_D		5.4	6.71	5.44
III (4.31 Å)	$x^{\neq}$ (Å)	.400		.000	.707
	$y^{\neq}$ (Å)	.725		.609	.587

Within the present work, the effect of accounting for repulsive interactions upon the saddle point coordinates is smallest for sites *I* and largest for sites *III*.

The system *III* NET is unusual in exhibiting a linear configuration of the critical system: the saddle point is found at $x=0$, *i. e.* in the surface plane of the metal.   Upon introduction of allowance for the repulsive effects of underlying metal atoms other than Ni(1) and Ni(2), a "normal" saddle point is found (*III* MAE and HAE—here the critical complex is trapezoidal as in the other cases), but the activation energy, $E_A = E^{\neq} - E^I$, becomes prohibitively high.   This is because for sites *III*, the repulsive forces exerted by the substrate atoms are stronger in the critical state than in the initial state.   The reverse is true for sites *I*.

The repulsion exerted by the metal atoms on the critical system is revealed mainly in the $x^{\neq}$ coordinate, in other words, the system is lifted, as may be expected.   The repulsion exerted be the adsorbed hydrogen atoms is revealed mainly in the $y^{\neq}$ coordinate, and it is seen from table 4 that the critical complex is obtained at larger separations of the two hydrogen atoms, (H–H), of the system on sites *I*, but at smaller (H–H) separations on sites *II* and *III*.   Both kinds of repulsion raise the potential energy at the saddle point[*].

*)   The calculations are expected to yield a lower limit to the estimated effects because it is likely that the adsorbed hydrogen atoms nearest the reaction site will follow to some extent the (H–H), in the way skin draws towards the centre of a healing wound; they are thus nearer to (H–H) than assumed in the calculations, and will exert greater repulsions.—There are further, more fundamental reasons to assume that the calculated effects are a lower limit, *cf.* the work of TOYA[8].

Juro HORIUTI and Klaus MÜLLER

In the (111) plane on site *III*, the hydrogen atom effect leads to a basic change: The saddle point is reached only when the system moves already in the x-direction, and thus resembles the final system, whereas in all other cases, the saddle point is reached when the system moves in the y-direction, and thus does not resemble the final system. However, all cases not involving sites *I* (the 2.49 Å sites) are practically excluded from the reaction.

From the values for the activation energies, *i.e.* the differences in energy between the critical system and the initial system of adsorbed hydrogen atoms, one would conclude that the reaction on the 2.49 Å site is occurring less readily on the (111) plane, and that this is due to the stronger repulsive action of surrounding hydrogen atoms on the critical complex in this case, as compared to those of other planes. This is qualitatively in agreement with some of the experimental findings of PIONTELLI *et al.*[44] (solutions of HCl and HClO$_4$); however, direct comparison cannot be made quantitatively unless relative coverages for the individual crystal planes at a given overvoltage are also accounted for. This has been done by HORIUTI and KITA[4] who point out that the relative contributions of the various crystal planes change with overvoltage in different ways. Their calculations may have to be corrected for $D_{\text{Ni-Ni}}$. However, the current densities calculated after statistically analysing the probability of coverage by H of sites directly neighbouring the critical complex should still represent reliable estimates since the correction for $D_{\text{Ni-Ni}}$ would *not* affect much the *relative* magnitudes of i_+ (the unidirectional rate of the hydrogen evolution reaction) for the *same type* of sites on various crystal planes. Thus, except at extreme overvoltages, $\theta < 1$, and it is most probable that Ni(3) and Ni(4) (see, for example, figure 4) are *not* covered by H. Just these H atoms contribute most of the repulsive potential, therefore, the present results calculated at $\theta = 1$ represent an upper limit to the situation at practical coverages $\theta < 1$. This is discussed in more detail on page 173 of the work of HORIUTI and KITA.

2. The force constants

On sites *I*, the interaction of the critical complex with metal atoms other than Ni(1) and Ni(2) has little effect, while adsorbed hydrogen atoms (the cases HAE) cause significant deviations between the various lattice planes. On sites *II* and *III*, the differences in the effects between various lattice planes are significant both in the MAE and HAE cases.

Near-zero values for a_{xx} in the cases NET, sites *I* and *II*, constitute a valid check for the accuracy of saddle point location, which is quite critical for further calculations involving the saddle point coordinates. In the case

of NET *III*, the linear configuration of the critical complex constitutes a kind of degeneracy that vitiates the criterion; here, a_{xy} and $a_{\xi\eta}$ are zero.[*]

3. Vibrational frequencies

Qualitatively, the effects of metal and hydrogen atoms are the same as in the case of force constants. It is noted that in the cases of NET *I* and *II*, there is one real vibrational frequency that is two orders of magnitude smaller than all others. None such is found in the MAE and HAE cases, and thus the partition functions in the latter cases are drastically reduced.

4. Separation factors

With all the NET, MAE, and HAE cases, except HAE *III*, there is a *basic* trend of the separation factors to increase with the distance of separation of the Ni atoms forming the site. For sites *I*, the metal atom effect leads to higher, the hydrogen atom effect leads to lower separation factors; for sites *II* and *III*, both metal and hydrogen atom effects lead to lower values. All values of S_D are between 4.9 and 7, except for the one case where the system moves in the x-direction when the saddle point is reached (see above), *i. e.* the system HAE *III* on the (111) plane, where the separation factor is much lower, and one other case, MAE *III*, also on the (111) plane, where the separation factor is much higher; in this last case, the force constants and the vibrational frequencies are relatively much lower than in all other cases. Of course, in view of the high energies of activation for the reaction on sites other than the 2.49 Å site, this discussion is of academic interest only.

Of principal practical importance is the result, mentioned at the beginning of the discussion, that there are no theoretical grounds to doubt the validity of calculated separation factors for mechanistic considerations where, regarding the catalytic mechanism of hydrogen evolution, the effect of interactions of the critical complex with underlying metal atoms or, at higher coverages of the electrode with H, simultaneously adsorbed hydrogen atoms is concerned.

5. Action of catalysts

The present calculations have been carried out for the case of nickel. One should predict that, on any metal, the best catalytic action is afforded

---

[*] Consider the critical complex as a trapezoid, with a rotational position defined by an angle α. In the case of NET *III*, the trapezoid has degenerated to a linear configuration of points, and its potential energy has now rotational symmetry around the y-axis. If α is increased to $\alpha+\pi$, then $a_{xy}xy$ and $a_{\xi\eta}\xi\eta$ change their signs because both x and ξ change signs while both y and η remain the same. The rotational symmetry, then, requires that a_{xy} and $a_{\xi\eta}$ vanish. The term $a_{\zeta\zeta}\zeta^2$ is unaffected by the rotation, and so is $a_{\zeta\zeta}$.

Juro HORIUTI and Klaus MÜLLER

on sites for which the metal-metal distance of the catalytic sites in question does not differ appreciably from the equilibrium distance of the corresponding diatomic metal molecule, and that sites other than these do not afford good catalytic action for reactions such as hydrogen combination, because in this case, the formation of a metal-metal molecule, one of the premises of the present method, does not release sufficient energy. If, for geometric reasons, a catalytic reaction requires sites of the last-mentioned type, then its catalysis by a given material should best be improved by creation of surface alloys or compounds with equilibrium distances between their constituent atoms that differ from those of the individual base material.

A favourable action of the supporting material of very thin (essentially monatomic) catalyst layers is predicted for the case where such a support brings about sites with a spacing closer to the equilibrium distance in the diatomic catalyst molecule than any of the commonly exposed lattice sites in unsupported samples of this catalyst.

It should also be expected that the isotopic effects such as separation factors do not depend appreciably on the metal if the mechanism is of the type considered here; this conclusion arises from the present work (relatively small effect of D_{Ni-Ni} on S) and from that of BOCKRIS and SRINIVASAN[3] (who varied D_{Ni-H}).

Acknowledgments

The authors are grateful to Prof. T. NAKAMURA for setting up and testing the third computer programme and for other valuable assistance. They are also indebted to Dr. H. KITA for finding the work on the Ni_2 molecule (Ref. 6) and for his help throughout; and to Mr. T. NAGAYAMA, Miss T. KAWAI, and Miss A. HIRATSUKA for their help in the computer calculations. One of the authors (K. M.) was recipient of a Research Fellowship from Nihon Gakujutsu Shinko-kai (The Japan Society for the Promotion of Science), Tokyo, which is gratefully acknowledged, and he is also much obliged to the entire staff of the Research Institute for Catalysis, Hokkaido University, for making work and life, for him and his wife as foreigners in Japan, materially possible, interesting, and a pleasant, lasting experience.

Note added in proof. Sites of proper spacing that are not present on a regular exposed lattice plane could also be created by certain electrochemical, chemical, or mechanical methods of activation, for example reduction of oxide films or abrasion. The results of BONNEMAY et al.[45] are direct proof since in their work, known changes in lattice spacings have been produced by mechanical means, and have given appreciable changes in catalytic activity.

References

1) G. OKAMOTO, J. HORIUTI and K. HIROTA, Sci. Papers Inst. Phys. Chem. Res. Tokyo, **29**, 223 (1936).

2) J. HORIUTI and T. NAKAMURA, J. Chem, Phys., **18**, 395 (1950);
T. NAKAMURA, Shokubai (Sapporo), **6**, 1 (1950);
J. HORIUTI and T. NAKAMURA, This Journal **2**, 73 (1951).

3) J. O'M. BOCKRIS and S. SRINIVASAN, J. Electrochem. Soc., **111**, 858 (1964).

4) J. HORIUTI and H. KITA, This Journal **12**, 122 (1965).

5) N. ROSEN and S. IKEHARA, Phys. Rev., **43**, 5 (1933).

6) A. KANT, J. Chem. Phys., **41**, 1872 (1964).

7) H. EYRING, J. Amer. Chem. Soc., **53**, 2537 (1931).

8) T. TOYA, This Journal **6**, 308 (1958), **8**, 209 (1960).

9) *Constitution of Binary Alloys*, ed. M. HANSEN, McGraw-Hill, New York, 2nd ed., 1958, p. 1267.

10) J. TAFEL, Z. Physik. Chem., **34**, 187 (1900).

11) M. IKUSHIMA and S. AZAKAMI, Nippon Kagaku Zasshi, **59**, 40 (1938).

12) O. SEPALL and S. G. MASON, Can. J. Chem., **38**, 2024 (1960).

13) S. SRINIVASAN, *Dissertation*, University of Pennsylvania, Philadelphia, Pa., 1963; J. O'M. BOCKRIS and S. SRINIVASAN, J. Electrochem. Soc., **111**, 844 (1964).

14) W. S. BENEDICT, N. GAILAR and E. K. PLYLER, J. Chem. Phys., **24**, 1139 (1956).

15) W. F. LIBBY, J. Chem. Phys., **11**, 101 (1943).

16) J. HORIUTI, Trans. Symp. Electrode Processes Philadelphia, Pa., 1959, ed. E. YEAGER, Wiley, New York, 1961, p. 17.

17) J. HORIUTI, A. MATSUDA, M. ENYO and H. KITA, Proc. Australian Conf. Electrochem., 1st, Sydney and Hobart, 1963, ed. J. A. FRIEND, F. GUTMANN, and J. W. HAYES, Pergamon Press, 1965, p. 750.

18) J. HORIUTI, This Journal, **1**, 8 (1948).

19) *idem, ibid.*, **4**, 55 (1956).

20) H. KITA and T. YAMAZAKI, *ibid.*, **11**, 10 (1963).

21) J. HORIUTI, *ibid.*, **11**, 164 (1964).

22) A. HICKLING and F. W. SALT, Trans. Faraday Soc., **38**, 474 (1942).

23) A. MATSUDA and J. HORIUTI, This Journal., **6**, 231 (1958).

24) J. HORIUTI and H. KITA, *ibid.*, **12**, 1, 14 (1964).

25) H. KITA and O. NOMURA, *ibid.*, **12**, 107 (1965).

26) M. I. TEMKIN, Zh. Fiz. Khim., **15**, 296 (1941).

27) J. HORIUTI and K. HIROTA, This Journal, **8**, 51, 167 (1960).

28) J. HORIUTI, *ibid.*, **9**, 143 (1961).

29) J. HORIUTI, Pure Appl. Chem., **5**, 641 (1962).

30) J. HORIUTI and T. TOYA, Kinetika i Kataliz, **4**, 3 (1963).

31) J. HORIUTI and T. TOYA, This Journal, **12**, 76 (1965).

32) K. J. VETTER, *Electrochemical Kinetics*, Academic Press, New York, 1967, p. 578.

33) F. HABER and R. RUSS, Z. Physik. Chem., **47**, 257 (1904).

Juro HORIUTI and Klaus MÜLLER

34) J. TAFEL, Z. Physik. Chem., **50**, 641 (1905).

35) A. WHEELER, quoted by O. BEECK, Rev. Mod. Phys., **17**, 61 (1945).

36) O. BEECK, Advan. Catalysis, **2**, 151 (1950) ;

O. BEECK, Discussions Faraday Soc., **8**, 118 (1950).

37) J. HORIUTI and T. TOYA, This Journal, **11**, 84 (1963).

38) A. MATSUDA, *ibid.*, **8**, 151 (1960).

39) B. E. CONWAY and E. GILEADI, Trans. Faraday Soc., **58**, 2493 (1962).

40) T. TOYA, This Journal, **10**, 236 (1962) ;

idem, Progr. theor. Phys. (Kyoto), Suppl., **23**, 250 (1963).

41) J. HORIUTI and G. OKAMOTO, Sci. Papers Inst. Phys. Chem. Res. Tokyo, **28**, 231 (1936).

42) B. E. CONWAY, Proc. Roy. Soc. (London), Ser. A, **247**, 400 (1958).

43) J. O'M. BOCKRIS and D. F. A. KOCH, J. Phys. Chem., **65**, 1941 (1961).

44) R. PIONTELLI, L. P. BICELLI and A. LA VECCHIA, WADD Technical Report 60–769, Feb. 1961 ;

R. PIONTELLI, L. P. BICELLI and A. LA VECCHIA, Atti Accad. Naz. Lincei, Rend., Classe Sci. Fis. Mat. Nat., [8] **27**, 312 (1959).

45) M. BONNEMAY, G. BRONOËL, E. LEVART and G. PESLERBE, Comptes rendus, Deuxièmes Journées Internationales d'Etude des Piles à Combustible, p. 27 (Brussels, 1967).